

Steering of vortices by magnetic-field tilting in superconductor nanotubes

Igor Bogush,^{1,2} Oleksandr V. Dobrovolskiy,³ and Vladimir M. Fomin^{1,2, a)}

¹⁾Institute for Emerging Electronic Technologies, Leibniz IFW Dresden, Helmholtzstraße 20, 01069 Dresden, Germany

²⁾Moldova State University, Str. A. Mateevici 60, 2009 Chişinău, Republic of Moldova

³⁾University of Vienna, Faculty of Physics, Nanomagnetism and Magnonics, Superconductivity and Spintronics Laboratory, Währinger Str. 17, 1090 Vienna, Austria

(Dated: 2 January 2024)

In planar superconductor thin films, the places of nucleation and arrangements of moving vortices are determined by structural defects. However, various applications of superconductors require reconfigurable steering of fluxons, which is hard to realize with geometrically predefined vortex pinning landscapes. Here, on the basis of the time-dependent Ginzburg-Landau equation, we present an approach for steering of vortex chains and vortex jets in superconductor nanotubes containing a slit. The idea is based on tilting of the magnetic field \mathbf{B} at an angle α in the plane perpendicular to the axis of a nanotube carrying an azimuthal transport current. Namely, while at $\alpha = 0^\circ$ vortices move paraxially in opposite directions within each half-tube, an increase of α displaces the areas with the close-to-maximum normal component $|B_n|$ to the close(opposite)-to-slit regions, giving rise to descending (ascending) branches in the induced-voltage frequency spectrum $f_U(\alpha)$. At lower B , upon reaching the critical angle α_c , close-to-slit vortex chains disappear, yielding f_U of the nf_1 -type ($n \geq 1$: an integer; f_1 : vortex nucleation frequency). At higher B , f_U is largely blurry because of multifurcations of vortex trajectories, leading to the coexistence of a vortex jet with two vortex chains at $\alpha = 90^\circ$. In addition to prospects for tuning of GHz-frequency spectra and steering of vortices as information bits, our findings lay foundations for on-demand tuning of vortex arrangements in 3D superconductor membranes in tilted magnetic fields.

Knowledge of how magnetic flux quanta (Abrikosov vortices) move and arrange themselves under various currents and magnetic fields is critical for supercurrent flow and fluxonic applications. For instance, while for defect-free planar thin films a hexagonal vortex lattice¹ is expected, sample defects and its geometry make vortex patterns to differ from a regular lattice²⁻⁴. In planar thin films, the places of nucleation of vortices are determined by edge defects⁵⁻⁷, current-crowding effects⁸⁻¹⁰ or their combinations¹¹⁻¹³. For structures with perfect edges, a single edge defect acts as a local injector of vortices¹⁴. Driven by the competing current-vortex and vortex-vortex interactions, such vortices form a jet which is narrow at the defect and *expands* due to the repulsion of vortices as they move to the opposite edge of the structure¹⁵.

An extension of a planar film into 3D brings about inhomogeneity¹⁶⁻¹⁹ of the normal-to-the-surface component $|B_n|$ of the applied magnetic field of induction \mathbf{B} , such that vortices nucleate and move in the regions where $|B_n|$ is maximal²⁰. In this regard, of particular interest are open superconductor nanotubes (with a slit), see Fig. 1, in which, under an azimuthal transport current, vortices are constrained to move within the half-tubes and vortex jets are *non-expanding*²¹. Previously, correlated dynamics of vortices in open nanotubes were investigated numerically with foci on pinning²², ac drives²³, topological transitions²⁴, and transient regimes²⁵. These predictions can be examined for, e.g., open Nb nanotubes fabricated by the self-rolling technology²⁶⁻²⁸. However, while the average induced voltage U and its frequency spectrum f_U contain information on the vortex arrangements²¹, the effects of magnetic-field tilting on their stability and transitions between these arrangements have not been investigated so far.

Here, we present an approach for steering of vortices in open superconductor nanotubes by tilting the vector \mathbf{B} at an angle α in the plane perpendicular to the nanotube axis. The numerical modeling is based on the time-dependent Ginzburg-Landau (TDGL) equation. Distinct from $\alpha = 0^\circ$, when vortices move paraxially in opposite directions within each half-tube, an increase of α displaces the areas with close-to-maximum $|B_n|$ to the close(opposite)-to-slit regions, giving rise to descending (ascending) branches in $f_U(\alpha)$. At lower

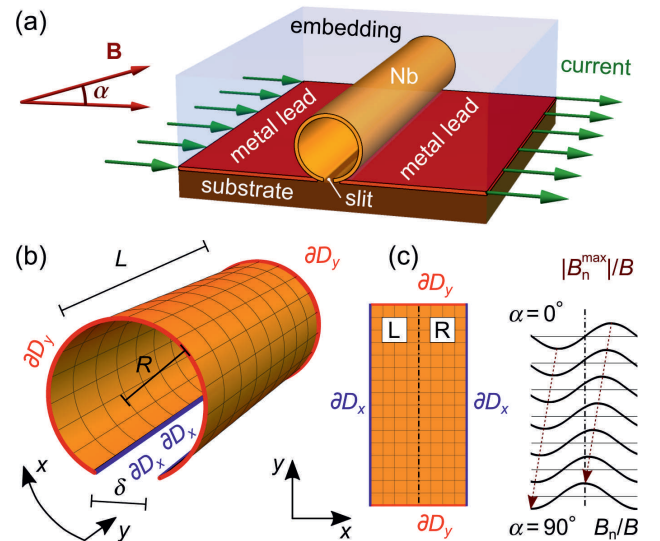


FIG. 1. Geometry (a) and the mathematical model (b) of an open nanotube. (c) Unwrapped view of the nanotube surface. Normally conducting current leads are attached to the slit banks and correspond to the ∂D_x boundaries. Indicated is also the evolution of the location of the $|B_n|$ maxima with increase of the magnetic field tilt angle α .

^{a)}Electronic mail: Vladimir M. Fomin, v.fomin@ifw-dresden.de

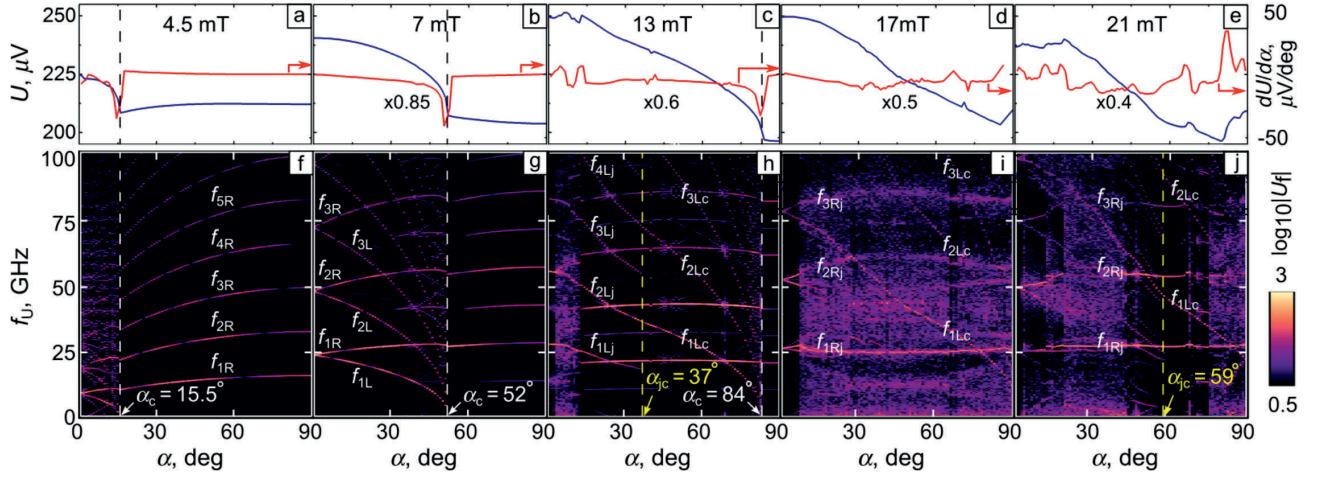


FIG. 2. (a-e) Average induced voltage U and (f-j) its frequency spectrum f_U as functions of the magnetic-field-tilt angle α for the nanotube with $R = 390$ nm at the transport current density 16 GA/m^2 .

B , a critical angle α_c is revealed, at which the close-to-slit vortex chains disappear and f_U evolves to the nf_1 -type [$n \geq 1$: an integer, f_1 : vortex nucleation frequency]. At higher B , f_U is largely blurry, due to multifurcations of the vortex trajectories in the opposite-to-slit vortex jet moving in the reverse direction with respect to the close-to-slit vortex chains. In all, our findings have implications for tuning of GHz-frequency spectra in microwave applications and on-demand steering of vortices as information carriers.

The studied geometry is shown in Fig. 1(a). An open superconductor nanotube of length $L = 5 \mu\text{m}$, radius $R = 390$ nm, with a slit of width $\delta = 60$ nm, is exposed to an azimuthal transport current of density \mathbf{j}_{tr} . A magnetic field of induction \mathbf{B} is applied perpendicular to the tube axis at an angle α relative to the substrate plane, varying between 0° and 90° . Under the action of the transport current, vortices nucleate at the free edges [boundaries ∂D_y in Fig. 1(b)] of the tube, move along the tube axis, and denucleate at the opposite free edges. At $\alpha = 0^\circ$, the vortices in the opposite half-tubes move in reverse directions due to the sign reversal of B_n , see Fig. 1(c). In what follows, we refer to the vortex arrangements and the half-tubes as “R” (right) and “L” (left), see Fig. 1(c). With increase of α , the R maximum of B_n shifts towards the opposite-to-slit region, while the L maximum of $|B_n|$ shifts towards the L slit bank. This continues until two $|B_n|$ maxima occur just at the slit banks outside of the nanotube and the B_n maximum coincides with the middle of the nanotube surface at $\alpha = 90^\circ$.

The TDGL equation is solved for parameters typical for Nb films²⁹ and the film thickness $d = 50$ nm resulting in the correspondence of a current density of 1 GA/m^2 to a transport current of 0.25 mA. Details on the equations and boundary conditions are provided elsewhere²¹. The modeling is performed for $j_{\text{tr}} = 16 \text{ GA/m}^2$ at temperature $T/T_c = 0.952$, where T_c is the superconducting transition temperature.

Figure 2 presents the average induced voltage U , its derivative with respect to the magnetic-field-tilt angle α , and the induced-voltage frequency spectrum f_U as functions of α for a series of magnetic field values. At lower fields (4.5-13 mT),

as α increases, $f_U(\alpha)$ manifests an abrupt transition from a regime with crossing ascending and descending branches to a regime of nf_1 -harmonics of the vortex nucleation frequency f_1 . The transitions occur at some critical angle α_c , which increases with increase of B . At the same time, $U(\alpha)$ manifests a sharp bend at $\alpha \lesssim \alpha_c$, while $dU/d\alpha$ exhibits a minimum at α_c . Whereas $f_U(\alpha)$ decreases for $\alpha < \alpha_c$, it slowly increases for $\alpha > \alpha_c$ at $\lesssim 7$ mT and is almost constant for $\gtrsim 7$ mT. At higher fields (17-21 mT), f_U is blurry, though one can recognize constant-frequency and descending branches. Overall, $U(\alpha)$ decreases by about 20% as α increases from 0° to 90° .

Further insights into the features of $f_U(\alpha)$ can be gained from the analysis of the spatial evolution of the absolute value of the superconducting order parameter $|\psi|$ as functions of α and B . Indeed, the evolution of U and f_U at 4.5 mT and 7 mT can be understood with the aid of the snapshots of $|\psi|(x, y)$ overlaid with the accumulated vortex trajectories in Fig. 3. Thus, at 7 mT and $\alpha = 0^\circ$, the vortices are arranged in two chains located symmetrically relative to the (dash-dotted) midline. At $\alpha = 0^\circ$, the intervortex distances in the L and R chains are equal, $a_L = a_R$. A tilt of \mathbf{B} by 15° leads to the inequality $a_R < a_L$, which becomes more pronounced with $a_L \simeq 3a_R$ at $\alpha = 45^\circ$. While the vortex velocities in the R and L half-tubes remain almost equal to each other, the vortex nucleation frequencies in the R and L half-tubes differ by a factor of $f_{\text{R}}/f_{\text{L}} \simeq 3$. This ratio agrees well with the frequency ratio $f_{1\text{R}}/f_{1\text{L}}$ at $\alpha = 45^\circ$ in Fig. 2(g).

At 7 mT, upon reaching the critical angle $\alpha_c = 52^\circ$, the L vortex chain disappears, decisively affecting the spectrum f_U . Namely, for angles $(\alpha_c - \alpha)/\alpha_c \ll 1$, the branches $nf_{1\text{L}}$ descend very rapidly and $U(\alpha)$ manifests a fast decrease, see Fig. 2(b). For $\alpha > \alpha_c$, the spectrum is of the $nf_{1\text{R}}$ -type. Herein, $f_{1\text{R}}$ are associated with the harmonics of the vortex nucleation frequency in the single L chain which is displaced to the opposite-to-slit area (midline), see Fig. 3(q). The vortex arrangements at 4.5 mT are qualitatively similar, but differ by a smaller number of vortices and a smaller α_c .

At 13 mT and for $\alpha = 0^\circ$, there are two vortex jets each

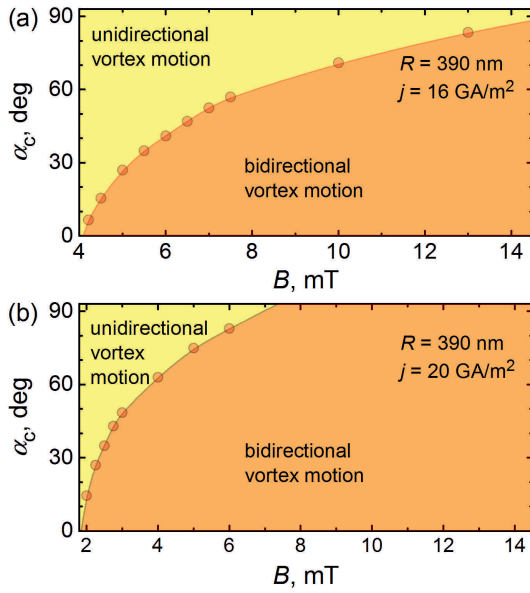


FIG. 4. The critical angle α_c as a function of the magnetic field at $j_{tr} = 16 \text{ GA/m}^2$ (a) and $j_{tr} = 20 \text{ GA/m}^2$ (b), demarcating the regimes of unidirectional and bidirectional vortex motion.

Finally, we would like to comment on a possible experimental examination and the general relevance of the obtained results. We note that deviations of \mathbf{B} by an angle α of few degrees from the perpendicular-to-tube-axis and parallel-to-substrate direction may easily occur in experiments²⁸, so transitions in f_U could be useful for checking the sample/field alignment. In addition, the evolution of vortex arrangements with increase of α is interesting from the viewpoint of both, basic research^{30,31} and emerging functionalities. For the tubes studied here, it is the steering of vortex arrays to desired parts of the nanotube via magnetic-field tilting and vortex-jet-to-vortex-chain transitions, which do not occur in planar thin films at moderately strong transport currents^{13,15}. Conceptually, steering of vortex chains, vortex jets and more complex arrangements is similar to using a magnetic field for controlling the vortex dynamics³², but surpasses vortex guiding in nanoengineered pinning landscapes in terms of reconfigurability^{33–35}. While spatio- and time-resolved studies of vortex arrangements in 3D nanoarchitectures are challenging, deduction of their properties from features in the global observables U and f_U represents a viable approach to that end.

IB is grateful to Victor Ciobu for technical support, including the generous provision of several servers that were instrumental for the calculations. OVD acknowledges the Austrian Science Fund (FWF) for support through Grant No. I 6079 (FluMag). VMF expresses his thanks to the European Cooperation in Science and Technology for support via Grant E-COST-GRANT-CA21144-d8436ac6-b039a83c-fa29-11ed-9946-0a58a9feac02 and to the ZIH TU Dresden for providing its facilities for high throughput calculations. This article is based upon work supported by the E-COST via Action CA21144 (SuperQuMap).

- ¹E. H. Brandt, *Rep. Progr. Phys.* **58**, 1465 (1995).
- ²C. Reichhardt, C. J. Olson, and F. Nori, *Phys. Rev. Lett.* **78**, 2648 (1997).
- ³I. Guillamón, H. Suderow, A. Fernández-Pacheco, J. Sesé, R. Córdoba, J. M. De Teresa, M. R. Ibarra, and S. Vieira, *Nature Physics* **5**, 651 (2009).
- ⁴A. V. Silhanek, M. V. Milošević, R. B. G. Kramer, G. R. Berdiyrov, J. Van de Vondel, R. F. Lucas, T. Puig, F. M. Peeters, and V. V. Moshchalkov, *Phys. Rev. Lett.* **104**, 017001 (2010).
- ⁵D. Cerbu, V. N. Gladilin, J. Cuppens, J. Fritzsche, J. Tempere, J. T. Devreese, V. V. Moshchalkov, A. V. Silhanek, and J. Van de Vondel, *New J. Phys.* **15**, 063022 (2013).
- ⁶B. Budinská, B. Aichner, D. Y. Vodolazov, M. Y. Mikhailov, F. Porrati, M. Huth, A. Chumak, W. Lang, and O. Dobrovolskiy, *Phys. Rev. Appl.* **17**, 034072 (2022).
- ⁷D. Y. Vodolazov, K. Ilin, M. Merker, and M. Siegel, *Supercond. Sci. Technol.* **29**, 025002 (2015).
- ⁸J. R. Clem and K. K. Berggren, *Phys. Rev. B* **84**, 174510 (2011).
- ⁹O.-A. Adami, D. Cerbu, D. Cabosart, M. Motta, J. Cuppens, W. A. Ortiz, V. V. Moshchalkov, B. Hackens, R. Delamare, J. Van de Vondel, and A. V. Silhanek, *Appl. Phys. Lett.* **102**, 052603 (2013).
- ¹⁰L. Embon, Y. Anahory, Z. L. Jelic, E. O. Lachman, Y. Myasoedov, M. E. Huber, G. P. Mikitik, A. V. Silhanek, M. V. Milosevic, A. Gurevich, and E. Zeldov, *Nat. Commun.* **8**, 85 (2017).
- ¹¹M. Friesen and A. Gurevich, *Phys. Rev. B* **63**, 064521 (2001).
- ¹²S. S. Ustavschikov, M. Y. Levichev, I. Y. Pashenkin, N. S. Gusev, S. A. Gusev, and D. Y. Vodolazov, *JETP Lett.* **135**, 226 (2022).
- ¹³V. Bevz, M. Mikhailov, B. Budinská, S. Lamb-Camarena, S. Shpilinska, A. Chumak, M. Urbánek, M. Arndt, W. Lang, and O. Dobrovolskiy, *Phys. Rev. Appl.* **19**, 034098 (2023).
- ¹⁴A. Aladyshkin, A. S. Mel'nikov, I. A. Shereshevsky, and I. D. Tokman, *Physica C* **361**, 67 (2001).
- ¹⁵A. I. Bezuglyj, V. A. Shklovskij, B. Budinská, B. Aichner, V. M. Bevz, M. Y. Mikhailov, D. Y. Vodolazov, W. Lang, and O. V. Dobrovolskiy, *Phys. Rev. B* **105**, 214507 (2022).
- ¹⁶A. R. de C. Romaguera, M. M. Doria, and F. M. Peeters, *Phys. Rev. B* **76**, 020505 (2007).
- ¹⁷J. Tempere, V. N. Gladilin, I. F. Silvera, J. T. Devreese, and V. V. Moshchalkov, *Phys. Rev. B* **79**, 134516 (2009).
- ¹⁸V. N. Gladilin, J. Tempere, J. T. Devreese, and V. V. Moshchalkov, *Phys. Rev. B* **86**, 104508 (2012).
- ¹⁹V. M. Fomin and O. V. Dobrovolskiy, *Appl. Phys. Lett.* **120**, 090501 (2022).
- ²⁰V. M. Fomin, R. O. Rezaev, and O. G. Schmidt, *Nano Lett.* **12**, 1282 (2012).
- ²¹I. Bogusch, O. V. Dobrovolskiy, and V. M. Fomin, arXiv:2311.02946.
- ²²R. H. De Braganca, I. Bogusch, and V. M. Fomin, arXiv:2312.xxxx.
- ²³V. M. Fomin, R. O. Rezaev, and O. V. Dobrovolskiy, *Sci. Rep.* **12**, 10069 (2022).
- ²⁴R. O. Rezaev, E. I. Smirnova, O. G. Schmidt, and V. M. Fomin, *Comm. Phys.* **3**, 144 (2020).
- ²⁵I. Bogusch and V. M. Fomin, *Phys. Rev. B* **105**, 094511 (2022).
- ²⁶D. J. Thurmer, C. Deneke, and O. G. Schmidt, *J. Phys. D: Appl. Phys.* **41**, 205419 (2008).
- ²⁷D. J. Thurmer, C. C. B. Bufon, C. Deneke, and O. G. Schmidt, *Nano Lett.* **10**, 3704 (2010).
- ²⁸S. Lösch, A. Alfonsov, O. V. Dobrovolskiy, R. Keil, V. Engemaier, S. Bannack, G. Li, O. G. Schmidt, and D. Bürger, *ACS Nano* **13**, 2948 (2019).
- ²⁹O. V. Dobrovolskiy and M. Huth, *Thin Solid Films* **520**, 5985 (2012).
- ³⁰C. J. Olson, C. Reichhardt, and F. Nori, *Phys. Rev. B* **56**, 6175 (1997).
- ³¹A. Glatz, V. K. Vlasko-Vlasov, W. K. Kwok, and G. W. Crabtree, *Phys. Rev. B* **94**, 064505 (2016).
- ³²M. Velez, J. I. Martin, J. E. Villegas, A. Hoffmann, E. M. Gonzalez, J. L. Vicent, and I. K. Schuller, *J. Magn. Magnet. Mat.* **320**, 2547 (2008).
- ³³F. A. Staas, A. K. Niessen, W. F. Druyvesteyn, and J. v. Suchtelen, *Phys. Lett.* **13**, 293 (1964).
- ³⁴A. V. Silhanek, J. Van de Vondel, and V. V. Moshchalkov, “Guided vortex motion and vortex ratchets in nanostructured superconductors,” in *Nanoscience and Engineering in Superconductivity* (Springer-Verlag, Berlin, 2010) Chap. 1, pp. 1–24.
- ³⁵O. Dobrovolskiy, E. Begun, V. Bevz, R. Sachser, and M. Huth, *Phys. Rev. Appl.* **13**, 024012 (2020).